Organic−Inorganic Hybrids Based on Polyoxometalates. 5.[1] Synthesis and Structural Characterization of Bis(organophosphoryl)decatungstosilicates [γ-$SiW_{10}O_{36}((RPO)_2]^{4-}$

Cédric R. Mayer, Patrick Herson, and René Thouvenot*

Laboratoire de Chimie Inorganique et Matériaux Moléculaires, Unité CNRS 7071, case courrier 42, Université Pierre et Marie Curie, 4 place Jussieu, F75252 Paris Cedex 05, France

Received June 22, 1999

Organophosphoryl polyoxotungstate derivatives [γ-$SiW_{10}O_{36}(RPO)_2]^{4-}$ (R = H (**1**), Et (**2**), *n*-Bu (**3**), *t*-Bu (**4**), C_2H_4COOH (**5**), Ph (**6**)) have been obtained by reaction of the divacant [γ-$SiW_{10}O_{36}]^{8-}$ anion with organophosphonic acids $RPO(OH)_2$ in acetonitrile. These new heteropolyanions have been characterized by elemental analysis, infrared spectroscopy, multinuclear (^{1}H, ^{29}Si, ^{31}P, and ^{183}W) NMR, and X-ray crystallography. Crystals of $(NBu_4)_2$-$(NEt_4)H[\gamma$-$SiW_{10}O_{36}(C_6H_5PO)_2]$ (anion **6**) are monoclinic, space group $P2_1$, with lattice constants $a = 16.489(4)$ Å, $b = 14.016(3)$ Å, $c = 18.542(8)$ Å, $\beta = 91.30(3)°$, and $Z = 2$. The hybrid anion has a structure of virtual C_{2v} symmetry with two phenylphosphonate groups grafted to the surface of the divacant tungstosilicate. ^{183}W and ^{31}P NMR spectra of NBu_4 salts in DMF solution agree with the solid-state structure and the virtual C_{2v} symmetry.

Introduction

Current interest for derivatized polyoxometalates (POMs) originates from the fundamental interest of modeling catalysis by metal oxides as well as from potential interesting applications in different fields such as bifunctional catalysis and antiviral and antitumoral chemotherapy.[2] In the case of organic and organometallic derivatives the properties of the polyoxometalate framework may be finely tuned by appropriate choice of the addenda group, and chiral organic groups may lead to asymmetric synthesis.[3] Moreover organic moieties with functionalized (polymerizable) groups may direct the formation of hybrid organic−inorganic materials. In the frame of this strategy our group is primarily concerned with the reactivity of organochlorosilanes $RSiCl_3$[4,5] and organophosphonic acids $RPO(OH)_2$[6] toward plurivacant polyoxotungstates. Organosilanes react with trivacant Keggin tungstate anions $[X^{n+}W_9O_{34}]^{(14-n)-}$ (X^{n+} = Si^{4+}, Ge^{4+}, P^{5+}, As^{5+}) to yield either $[XW_9O_{34}(t\text{-BuSiOH})_3]^{(8-n)-}$ or $[XW_9O_{34}(RSiO)_3(RSi)]^{(8-n)-}$ ($R \neq t$-Bu). In all these hybrid anions, three RSi groups are grafted on the polyoxometalate via six Si−O−W bridges, resulting in the saturation of the POM surface.

The reactivity of $RSnCl_3$ with plurivacant polyoxotungstates was investigated by Pope et al.[7] The formation of saturated organotin(IV) derivatives with markedly different structures is explained by the preference of Sn(IV) to expand its coordination sphere. Actually, octahedrally coordinated tin atoms are embedded between two polyoxometalates units in $[(\beta$-A-$PW_9O_{34})_2$-$(PhSnOH)_3]^{12-}$,[7a] $[(\alpha$-A-$SiW_9O_{34})_2(BuSnOH)_3]^{12-}$,[7b] and $[(\gamma$-$SiW_{10}O_{36})_2(PhSnOH_2)_2]^{10-}$,[7c] whereas tin pentacoordination is reached in $[(\beta$-A-$SiW_9O_{34})(BuSnO)_3]^{7-}$.[7b]

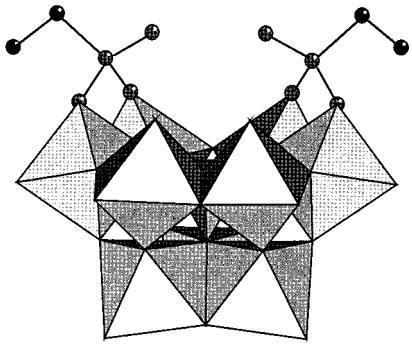

Figure 1. Polyhedral representation of $[PW_9O_{34}(RPO)_2]^{5-}$.

We recently investigated the reactivity of organophosphonic acids with trivacant Keggin anions. Hybrid derivatives $[PW_9O_{34}$-$(RPO)_2]^{5-}$ were obtained (Figure 1), where only two electrophilic groups RPO^{2+} are grafted on the polyoxometalate which therefore remains unsaturated.[6]

In a previous paper about monovacant tungstosilicate and -phosphate Kim et al. reported the formation of $[X^{n+}W_{11}O_{39}$-$(PhPO)_2]^{(8-n)-}$ with two organophosphoryl groups saturating the lacuna.[8]

We present here the study of the reaction of organophosphonic acids $RPO(OH)_2$ (R = H, Et, *n*-Bu, *t*-Bu, C_2H_4COOH, Ph) with the divacant anion [γ-$SiW_{10}O_{36}]^{8-}$, which presents as well four nucleophilic surface oxygen atoms. The hybrid anions have

* Corresponding author. E-mail: rth@ccr.jussieu.fr.

(1) Part 4: Alloul, L.; Ammari, N.; Mayer, C. R.; Mazeaud, A.; Thouvenot, R. *J. Chim. Phys.* **1998**, *95*, 289.
(2) For reviews on POM, see: (a) Pope, M. T. *Heteropoly and Isopoly Oxometalates*; Springer-Verlag: Berlin, New York, 1983. (b) Pope, M. T.; Müller, A. *Angew. Chem., Int. Ed. Engl.* **1991**, *30*, 34. (c) *Polyoxometalates: From Platonic Solids to Antiretroviral Activity*; Pope, M. T., Müller, A., Eds.; Kluwer Academic Publishers: Dordrecht, The Netherlands, 1994. (d) *Chem. Rev.* **1998**, *98*, 1−390 (special issue devoted to polyoxometalates; Hill, C. L., guest editor).
(3) Gouzerh, P.; Proust, A. *Chem. Rev.* **1998**, *98*, 77.
(4) (a) Ammari, N.; Hervé, G.; Thouvenot, R. *New. J. Chem.* **1991**, *15*, 607. (b) Ammari, N. Ph.D. Thesis, Université Pierre et Marie Curie, 1991.
(5) (a) Mazeaud, A.; Ammari, N.; Robert, F.; Thouvenot, R. *Angew. Chem., Int. Ed. Engl.* **1996**, *35*, 1961. (b) Mazeaud, A. Ph.D. Thesis, Université Pierre et Marie Curie, 1997.
(6) Mayer, C. R.; Thouvenot, R. *J. Chem. Soc., Dalton Trans.* **1998**, 7.
(7) (a) Xin, F.; Pope, M. T. *Organometallics.* **1994**, *13*, 4881. (b) Xin, F.; Pope, M. T.; Long, G. J.; Russo, U. *Inorg. Chem.* **1996**, *35*, 1207. (c) Xin, F.; Pope, M. T. *Inorg. Chem.* **1996**, *35*, 5693.
(8) Kim, G. S.; Hill, C. L. *Inorg. Chem.* **1992**, *31*, 5316.

10.1021/ic990724f CCC: $18.00
Published on Web 12/09/1999

been thoroughly characterized by spectroscopic methods (IR, multinuclear NMR) and by X-ray crystallography.

Experimental Section

Synthesis. Potassium γ-tungstosilicate $K_8[\gamma\text{-}SiW_{10}O_{36}]\cdot 12H_2O$ was synthesized according to Canny et al.,[9] and its purity was checked by IR spectroscopy and polarography. All other reagents and solvents are from commercial sources and were used as received.

$(NBu_4)_3K[\gamma\text{-}SiW_{10}O_{36}(HPO)_2]$ (Mixed Salt of Anion 1). Powdered $K_8[\gamma\text{-}SiW_{10}O_{36}]\cdot 12H_2O$ (12 g, 4 mmol) was suspended in an acetonitrile solution (200 mL) of NBu_4Br (3.9 g, 12 mmol) and $HPO(OH)_2$ (0.65 g, 8 mmol). A 12 M hydrochloric acid solution (1.33 mL) was poured dropwise under vigorous stirring, and the mixture was stirred overnight at reflux. After separation of the white residue (KBr + a small amount of unreacted SiW_{10}), the white compound $(NBu_4)_3K[\gamma\text{-}SiW_{10}O_{36}(HPO)_2]$ was obtained by evaporation of the resulting solution in a rotary evaporator. The crude compound was washed with distilled water and recrystallized from DMF or acetonitrile. Yield: 9.2 g (2.78 mmol, 70%). Anal. Calcd for $C_{48}H_{110}KN_3O_{38}P_2SiW_{10}$: C, 17.44; H, 3.35; K, 1.18; N, 1.27; P, 1.87; Si, 0.85; W, 55.63. Found: C, 18.20; H, 3.25; K, 1.14; N, 1.33; P, 1.92; Si, 0.90; W, 55.00. ^{1}H NMR (CD_3CN): δ 7.04 (2H, d, $^1J_{P-H}$ = 728 Hz). ^{31}P NMR (DMF/acetone-d_6): δ 4.4 (d, $^1J_{P-H}$ = 731 Hz, $^2J_{W-P}$ = 9.5 Hz). See Table 5 for ^{183}W NMR parameters.

$(NBu_4)_3K[\gamma\text{-}SiW_{10}O_{36}(EtPO)_2]$ (mixed salt of anion 2) was prepared and purified analogously using the same quantities as above with $EtPO(OH)_2$ (0.88 g, 8 mmol). Yield: 9.0 g (2.68 mmol, 67%). Anal. Calcd for $C_{52}H_{118}KN_3O_{38}P_2SiW_{10}$: C, 18.58; H, 3.54; K, 1.16; N, 1.25; P, 1.84; Si, 0.84; W, 54.7. Found: C, 19.20; H, 3.61; K, 1.22; N, 1.30; P, 1.80; Si, 0.86; W, 55.2. ^{1}H NMR (CD_3CN): δ 0.67 (6H, m), 1.24 (4H, m). ^{13}C{H} NMR (CD_3CN): δ 20.67 (2C, d, $^1J_{P-C}$ = 152.7 Hz), 6.65 (2C, d, $^2J_{P-C}$ = 6.72 Hz). ^{29}Si NMR (DMF/acetone-d_6): δ −85.93. ^{31}P{^{1}H} NMR (DMF/acetone-d_6): δ 32.7 ($^2J_{W-P}$ = 9.7 Hz). See Table 5 for ^{183}W NMR parameters.

$(NBu_4)_3K[\gamma\text{-}SiW_{10}O_{36}(n\text{-}BuPO)_2]$ (mixed salt of anion 3) was prepared and purified analogously using the same quantities as above with n-$BuPO(OH)_2$ (1.1 g, 8 mmol). Yield: 8.9 g (2.6 mmol, 65%). Anal. Calcd for $C_{56}H_{126}KN_3O_{38}P_2SiW_{10}$: C, 19.68; H, 3.72; K, 1.14; N, 1.23; P, 1.81; Si, 0.82; W, 53.8. Found: C, 18.10; H, 4.10; K, 1.17; N, 1.22; P, 1.85; Si, 0.84; W, 53.95. ^{1}H NMR (CD_3CN): δ 0.86 (6H, t), 1.18 (4H, m), 1.27 (4H, m), 1.35 (4H, m). ^{13}C{^{1}H} NMR (CD_3CN): δ 27.04 (2C, d, $^1J_{P-C}$ = 151.8 Hz), 22.90 (2C, d, $^2J_{P-C}$ = 8.2 Hz), 24.25 (2C, d, $^3J_{P-C}$ = 5.2 Hz), 13.40 ppm (2C, s). ^{31}P{^{1}H} NMR (DMF/acetone-d_6): δ 30.1 ($^2J_{W-P}$ = 9.8 Hz). See Table 5 for ^{183}W NMR parameters.

$(NBu_4)_3K[\gamma\text{-}SiW_{10}O_{36}(t\text{-}BuPO)_2]$ (mixed salt of anion 4) was prepared and purified analogously using the same quantities as above with t-$BuPO(OH)_2$ (1.1 g, 8 mmol). Yield: 8.5 g (2.49 mmol, 62%). Anal. Calcd for $C_{56}H_{126}KN_3O_{38}P_2SiW_{10}$: C, 19.68; H, 3.72; K, 1.14; N, 1.23; P, 1.81; Si, 0.82; W, 53.8. Found: C, 17.93; H, 4.05; K, 1.17; N, 1.21; P, 1.76; Si, 0.85; W, 54.65. ^{1}H NMR (CD_3CN): δ 0.9 (18H, s). ^{13}C{H} NMR (CD_3CN): δ 31.95 (2C, d, $^1J_{P-C}$ = 152.7 Hz), 24.88 ppm (6C, s). ^{29}Si NMR (DMF/acetone-d_6): δ −85.78. ^{31}P{^{1}H} NMR (DMF/acetone-d_6): δ 33.1 ($^2J_{W-P}$ = 9.5 Hz). See Table 5 for ^{183}W NMR parameters.

$(NBu_4)_3K[\gamma\text{-}SiW_{10}O_{36}(HOOCC_2H_4PO)_2]$ (mixed salt of anion 5) was prepared and purified analogously using the same quantities as above with $HOOCC_2H_4PO(OH)_2$ (1.23 g, 8 mmol). Yield: 8.3 g (2.4 mmol, 60%). Anal. Calcd for $C_{54}H_{118}KN_3O_{42}P_2SiW_{10}$: C, 18.8; H, 3.45; K, 1.13; N, 1.22; P, 1.80; Si, 0.81; W, 53.3. Found: C, 19.40; H, 3.60; K, 1.12; N, 1.31; P, 1.90; Si, 0.85; W, 54.5. ^{1}H NMR (CD_3CN): δ 9.4 (2H, s), 2.6 (4H, t), 1.7 (4H, m). ^{13}C{H} NMR (CD_3CN): δ 23.14 (2C, d, $^1J_{P-C}$ = 156.5 Hz), 27.28 (2C, d, $^2J_{P-C}$ = 2 Hz), 173.10 (2C, d, $^3J_{P-C}$ = 20.6 Hz). ^{29}Si NMR (DMF/acetone-d_6): δ −85.83. ^{31}P-{^{1}H} NMR (DMF/acetone-d_6): δ 27.9 ($^2J_{W-P}$ = 10.1 Hz). See Table 5 for ^{183}W NMR parameters.

(9) (a) Canny, J.; Tézé, A.; Thouvenot, R.; Hervé, G. *Inorg. Chem.* **1986**, *25*, 2114. (b) Tézé, A.; Hervé, G. *Inorg. Synth.* **1990**, *27*, 85.

Table 1. Crystallographic Data for $(NBu_4)_2(NEt_4)H[\gamma\text{-}SiW_{10}O_{36}(C_6H_5PO)_2]$

chem formula	$(NBu_4)_2(NEt_4)H[\gamma\text{-}SiW_{10}O_{36}(C_6H_5PO)_2]$
fw	3306
T, °C	25
λ, Å	0.710 69
cryst system	monoclinic
space group	$P2_1$
a, Å	16.489(4)
b, Å	14.016(3)
c, Å	18.542(8)
β, deg	91.30(3)
V, Å^3	4284(2)
Z	2
ρ_{calcd}, g cm^{-3}	2.56
μ, cm^{-1}	137.88
R^a	0.053
$R_w{}^b$	0.063
enantiopole param^c	0.03

^{a} $R = \sum||F_o| - |F_c||/\sum|F_o|$. ^{b} $R_w = [\sum w(|F_o| - |F_c|)^2/\sum wF_o^2]^{1/2}$. ^{c} $F_c = [(1-x)F(H)^2 + xF(-H)^2]^{1/2}$, $x = 0$ for correct and +1 for inverted absolute structures.

$(NBu_4)_3K[\gamma\text{-}SiW_{10}O_{36}(PhPO)_2]$ (mixed salt of anion 6) was prepared and purified analogously using the same quantities as above with $PhPO(OH)_2$ (1.26 g, 8 mmol). Yield: 9.2 g (2.7 mmol, 66.5%). Anal. Calcd for $C_{60}H_{118}KN_3O_{38}P_2SiW_{10}$: C, 20.85; H, 3.44; K, 1.13; N, 1.22; P, 1.79; Si, 0.81; W, 53.18. Found: C, 21.18; H, 3.49; K, 1.20; N, 1.28; P, 1.75; Si, 0.83; W, 53.45. ^{1}H NMR (CD_3CN): δ 8.3 (4H, m), 7.5 (6H, m). ^{13}C{H} NMR (CD_3CN): δ 132.9 (1C, d, $^1J_{P-C}$ = 151.5 Hz), 128.4 (2C, d, $^2J_{P-C}$ = 16.95 Hz), 130.4 (2C, d, $^3J_{P-C}$ = 8.5 Hz), 127.0 (s, 1C). ^{29}Si NMR (DMF/acetone-d_6): δ −85.59. ^{31}P{^{1}H} NMR (DMF/acetone-d_6): δ (15.3, $^2J_{W-P}$ = 11 Hz). See Table 5 for ^{183}W NMR parameters.

Obtention of Crystals for X-ray Analysis. Crystals of mixed (NBu_4^+/K^+) salts were all poorly diffracting and could not be used for X-ray structural determination. Suitable crystals were obtained with a mixture of tetraalkylammonium cations NEt_4^+ and NBu_4^+. The preparation of $(NEt_4)_3K$**[6]** was carried out by following a procedure strictly similar to that used for $(NBu_4)_3K$**[6]**, using NEt_4Br (2.5 g, 12 mmol). Crude $(NEt_4)_3K$**[6]** (1.0 g) and $(NBu_4)_3K$**[6]** (2.0 g) were dissolved in 60 mL of acetonitrile. Uncolored well-shaped single crystals of $(NBu_4)_2(NEt_4)H[\gamma\text{-}SiW_{10}O_{36}(PhPO)_2]$ which were used for crystallography studies were obtained after several days by slow evaporation of the solvent at room temperature.

Physical Measurements. Elemental analyses were performed by the "Service central de microanalyses du CNRS", Vernaison, France. Infrared spectra were recorded on a Bio-Rad FTS 165 IR FT spectrometer with compounds sampled in KBr pellets. ^{29}Si NMR spectra were obtained at room temperature in 10 mm o.d. tubes on a Bruker AM500 spectrometer. All other NMR spectra were obtained at room temperature on a Bruker AC300 spectrometer equipped with a QNP probehead (^{1}H, ^{13}C, and ^{31}P; 5 mm o.d. tubes) or a special low-frequency VSP probehead (^{183}W; 10 mm o.d. tubes). Resonance frequencies were 300.13, 75.46, 99.35, 121.5, and 12. 5 MHz for ^{1}H, ^{13}C, ^{29}Si, ^{31}P, and ^{183}W, respectively. Chemical shifts are reported according to the IUPAC convention, with respect to $SiMe_4$ (^{1}H, ^{13}C, ^{29}Si), 85% H_3PO_4 (^{31}P), and 2 M Na_2WO_4 alkaline aqueous solution (^{183}W). For ^{13}C and ^{1}H NMR the deuterated solvent CD_3CN ($\delta(^{13}CD_3)$ = 1.39 ppm) and its residual monoprotiated form CHD_2CN ($\delta(^1H)$ = 1.94 ppm) were used as internal secondary standards. For ^{29}Si, ^{31}P, and ^{183}W the chemical shifts were calibrated with external standards: in the case of ^{183}W a saturated D_2O solution of tungstosilicic acid, $H_4SiW_{12}O_{40}$, was used as secondary standard (δ −103.8 ppm). The ^{31}P-decoupled ^{183}W spectra were obtained using the Bruker B-SV3 unit equipped with a B-BM1 broad-band modulator. The output power of the modulated 121.5 MHz carrier was adjusted to about 5 W before entering the decoupling coil of the low-frequency probehead.

X-ray Crystallographic Study of $(NBu_4)_2(NEt_4)H$[6]. Lattice parameters were obtained from least-squares refinement of the setting angles of 27 reflections. The intensity data were collected at room

Table 2. Fractional Atomic Coordinates and U Values (Å^2) for $(NBu_4)_2(NEt_4)H[\gamma\text{-}SiW_{10}O_{36}(C_6H_5PO)_2]$

atom	*x*/*a*	*y*/*b*	*z*/*c*	*U*(eq)	atom	*x*/*a*	*y*/*b*	*z*/*c*	*U*(eq)
W(1)	0.3364(1)	0.3895(2)	0.40554(9)	0.0323	O(57)	0.195(1)	0.211(2)	0.436(1)	0.024(5)
W(2)	0.2831(1)	0.1088(2)	0.1820(1)	0.0307	O(58)	0.173(2)	0.091(2)	0.338(2)	0.038(7)
W(3)	0.2512(1)	0.2773(2)	0.06406(9)	0.0304	O(69)	0.106(2)	0.452(2)	0.086(1)	0.033(6)
W(4)	0.3034(1)	0.5584(2)	0.2878(1)	0.0336	O(78)	0.059(2)	0.224(2)	0.351(1)	0.028(6)
W(5)	0.2657(1)	0.1488(2)	0.37303(9)	0.0314	O(89)	0.064(2)	0.247(2)	0.207(1)	0.028(6)
W(6)	0.1965(1)	0.5143(2)	0.11900(9)	0.0310	O(100)	0.443(2)	0.395(2)	0.357(2)	0.045(7)
W(7)	0.1269(1)	0.3136(2)	0.40317(9)	0.0305	O(104)	0.194(2)	0.554(2)	0.307(2)	0.045(7)
W(8)	0.0959(1)	0.1511(2)	0.27475(9)	0.0284	O(106)	0.122(2)	0.577(2)	0.184(1)	0.038(7)
W(9)	0.0590(9)	0.3455(2)	0.13862(9)	0.0287	O(107)	0.091(1)	0.416(2)	0.342(1)	0.024(5)
W(10)	0.0886(1)	0.5084(2)	0.26689(9)	0.0306	O(109)	0.019(2)	0.432(2)	0.209(1)	0.031(6)
Si(1)	0.2376(6)	0.3345(7)	0.2444(5)	0.024(2)	O(111)	0.168(1)	0.401(1)	0.208(1)	0.017(5)
P(1)	0.4814(7)	0.4554(8)	0.2973(6)	0.042(3)	O(112)	0.193(1)	0.261(2)	0.304(1)	0.021(5)
P(2)	0.4376(7)	0.2192(8)	0.1104(6)	0.037(2)	O(114)	0.297(1)	0.403(2)	0.291(1)	0.020(5)
O(1)	0.373(2)	0.397(2)	0.492(2)	0.049(8)	O(123)	0.275(2)	0.269(2)	0.185(1)	0.029(6)
O(2)	0.298(2)	−0.013(2)	0.172(1)	0.031(6)	O(200)	0.420(2)	0.524(2)	0.268(1)	0.039(7)
O(3)	0.248(2)	0.273(2)	−0.025(2)	0.046(7)	O(300)	0.399(1)	0.148(2)	0.164(1)	0.028(5)
O(4)	0.320(2)	0.676(2)	0.293(2)	0.046(8)	O(400)	0.374(2)	0.275(2)	0.071(2)	0.043(7)
O(5)	0.312(2)	0.062(2)	0.426(2)	0.044(7)	O(1000)	0.521(2)	0.394(2)	0.242(2)	0.057(9)
O(6)	0.208(2)	0.596(2)	0.051(1)	0.032(6)	O(2000)	0.500(2)	0.280(2)	0.147(2)	0.054(8)
O(7)	0.071(2)	0.332(2)	0.478(1)	0.043(7)	C(1)	0.558(4)	0.531(4)	0.338(3)	0.06(1)
O(8)	0.020(2)	0.070(2)	0.266(2)	0.042(7)	C(2)	0.536(3)	0.596(4)	0.391(3)	0.05(1)
O(9)	−0.027(2)	0.319(2)	0.091(2)	0.038(7)	C(3)	0.596(4)	0.656(5)	0.426(3)	0.08(2)
O(10)	0.021(1)	0.592(2)	0.299(1)	0.029(6)	C(4)	0.666(5)	0.631(6)	0.413(4)	0.11(3)
O(14)	0.331(2)	0.528(2)	0.387(2)	0.049(8)	C(5)	0.697(4)	0.554(5)	0.366(4)	0.08(2)
O(15)	0.339(1)	0.256(1)	0.390(1)	0.017(5)	C(6)	0.630(4)	0.519(5)	0.320(4)	0.09(2)
O(17)	0.229(2)	0.388(2)	0.424(2)	0.043(7)	C(7)	0.485(3)	0.148(4)	0.042(3)	0.05(1)
O(23)	0.259(2)	0.145(2)	0.081(1)	0.034(6)	C(8)	0.573(4)	0.150(5)	0.049(3)	0.08(2)
O(25)	0.306(2)	0.124(2)	0.283(2)	0.041(7)	C(9)	0.610(3)	0.085(4)	−0.003(3)	0.07(1)
O(28)	0.173(2)	0.106(2)	0.201(2)	0.040(7)	C(10)	0.567(4)	0.029(5)	−0.056(4)	0.09(2)
O(36)	0.259(1)	0.413(2)	0.077(1)	0.020(5)	C(11)	0.483(4)	0.033(5)	−0.052(4)	0.08(2)
O(39)	0.145(2)	0.276(2)	0.084(1)	0.036(6)	C(12)	0.440(4)	0.091(5)	−0.004(4)	0.09(2)
O(46)	0.277(2)	0.549(2)	0.187(2)	0.037(7)					

[a] $U(\text{eq}) = (U_1U_2U_3)^{1/3}$; U_1, U_2, and U_3 are the principal axes of the thermal ellipsoids.

temperature with a $\theta-2\theta$ scan technique on an Enraf-Nonius CAD4 four-circle diffractometer, using graphite-monochromated Mo Kα radiation. Two standard reflections were measured periodically, and they showed no change during data collection. Crystallographic data and structure refinement parameters are listed in Table 1. Intensities were corrected for Lorentz−polarization effects, and an absorption correction was carried out using ψ-scan. All computations were performed by using the CRYSTALS version for PC.[10] Neutral-atom scattering factors for W, P, Si, C, N, and O were used, and real and imaginary parts of anomalous dispersion were taken into account.[11] The structure was solved by direct methods using the SHELX-86 program and successive difference Fourier maps.[12] Hydrogen contributions were omitted. Least-squares refinements with approximation in five blocks were carried out by minimizing the function $\sum w(|F_o| - |F_c|)^2$, where F_o and F_c are the observed and calculated structure factors, respectively. The model reached convergence with $R = \sum||F_o| - |F_c||/\sum|F_o|$ and $R_w = [\sum w(|F_o| - |F_c|)^2/\sum wF_o^2]^{1/2}$, having values of 0.053 and 0.063, respectively. Criteria for a satisfactory, complete analysis were the ratio of the root-mean-square shift to standard deviation being less than 0.1 and no significant features in the final difference map. Final atomic coordinates and thermal parameters of $(NBu_4)_2(NEt_4)H$-[**6**] are given in Table 2.

Results and Discussion

Synthesis and Characterization. The decatungstosilicate anion $[\gamma\text{-}SiW_{10}O_{36}]^{8-}$ [9] is the divacant lacunary derivative of the Keggin γ-isomer $[\gamma\text{-}SiW_{12}O_{40}]^{4-}$.[13] As removal of metal octahedra from a saturated polyoxometalate framework leads to increase and localization of the anionic charge, the resulting lacunary anion becomes highly nucleophilic and reacts easily with electrophilic groups. So, in the case of the trivacant heteropolyanion $[PW_9O_{34}]^{9-}$, two electrophilic groups RPO^{2+} graft to the polyoxotungstate surface, partially saturating the lacuna.[6] Similarily in the presence of the divacant heteropolyanion $[\gamma\text{-}SiW_{10}O_{36}]^{8-}$, the RPO^{2+} group acts as an electrophile and yields the fully saturated hybrid organic−inorganic species $[\gamma\text{-}SiW_{10}O_{36}(RPO)_2]^{4-}$. As for the hybrid organic−inorganic species $[PW_9O_{34}(RPO)_2]^{5-}$, the reaction proceeds under phase-transfer condition with a tetraalkylammonium cation $NR'_4{}^+$ (R′ = *n*-Bu or Et) (eq 1).

$$[\gamma\text{-}SiW_{10}O_{36}]^{8-} + 2RPO(OH)_2 + 4H^+ \xrightarrow[NR'_4Br]{MeCN} [\gamma\text{-}SiW_{10}O_{36}(RPO)_2]^{4-} + 4H_2O \quad (1)$$

R = H (**1**), Et (**2**), *n*-Bu (**3**), *t*-Bu (**4**), C_2H_4COOH (**5**), Ph (**6**)

All the spectroscopic data were gathered from the tetrabutylammonium salts after recrystallization from its DMF solutions. However all crystals were poorly diffracting and/or twined and could not be used for an X-ray structural determination. Suitable crystals were obtained successfully only when using a blending of alkylammonium salts. Indeed, the crystal submitted to X-ray diffraction analysis contains two tetrabutylammonium and one tetraethylammonium cations.

Structure of $(NBu_4)_2(NEt_4)H[\gamma\text{-}SiW_{10}O_{36}(C_6H_5PO)_2]$. A Cameron[14] view of **6** with the tungsten atom labeling scheme

(10) Watkin, D. J.; Carruthers, J. R.; Betteridge, P. W. *CRYSTALS, An Advanced Crystallographic Computer Program*; Chemical Crystallography Laboratory: Oxford, U.K., 1989.
(11) *International Tables For X-ray Crystallography*; Kynoch Press: Birmingham, England, 1974; Vol. IV.
(12) Sheldrick, G. M. *SHELXS-86, Program For Crystal Structure, Solution*; University of Göttingen: Göttingen, Germany, 1986.
(13) Tézé, A.; Canny, J.; Gurban, L.; Thouvenot, R.; Hervé, G. *Inorg. Chem.* **1996**, *35*, 1001.

Table 3. Selected Geometric Parameters for $(NBu_4)_2(NEt_4)H[\gamma\text{-}SiW_{10}O_{36}(C_6H_5PO)_2]$

atoms	dist, Å	atoms	dist, Å	atoms	dist, Å	atoms	dist, Å	mean values, Å
W(1)−O(1)	1.71(3)	W(2)− O(2)	1.74(2)	W(3)−O(3)	1.66(3)	W(4)−O(4)	1.67(3)	1.70
W(1) − O(14)	1.98(3)	W(2)−O(23)	1.97(3)	W(3)−O(23)	1.89(3)	W(4)−O(14)	1.93(3)	1.94
W(1)−O(15)	1.90(2)	W(2)−O(25)	1.92(3)	W(3)−O(36)	1.92(2)	W(4)−O(46)	1.92(3)	1.91
W(1)−O(17)	1.81(3)	W(2)−O(28)	1.86(3)	W(3)−O(39)	1.80(3)	W(4)−O(104)	1.85(3)	1.83
W(1)−O(114)	2.21(2)	W(2)−O(123)	2.25(2)	W(3)−O(123)	2.27(3)	W(4)−O(114)	2.19(2)	2.23
W(1)−O(100)	1.99(3)	W(2)−O(200)	2.02(2)	W(3)−O(300)	2.03(3)	W(4)−O(400)	2.03(3)	2.02
W(7)−O(7)	1.70(3)	W(8)−O(8)	1.69(3)	W(9)−O(9)	1.70(3)	W(10)−O(10)	1.74(2)	1.71
W(7)−O(17)	2.00(3)	W(8)−O(28)	1.99(3)	W(9)−O(39)	2.01(3)	W(10)−O(104)	1.98(3)	1.99
W(7)−O(57)	1.91(2)	W(8)−O(58)	1.90(3)	W(9)−O(69)	1.96(3)	W(10)−O(106)	1.91(3)	1.92
W(7)−O(107)	1.91(2)	W(8)−O(89)	1.91(2)	W(9)−O(89)	1.87(2)	W(10)−O(107)	1.91(2)	1.90
W(7)−O(78)	1.92(3)	W(8)−O(78)	1.86(2)	W(9)−O(109)	1.91(2)	W(10)−O(109)	1.89(3)	1.89
W(7)−O(112)	2.28(2)	W(8)−O(112)	2.28(2)	W(9)−O(111)	2.32(2)	W(10)−O(111)	2.28(2)	2.29
W(5)−O(5)	1.73(3)	W(6)−O(6)	1.71(2)					1.72
W(5)−O(57)	1.88(2)	W(6)−O(69)	1.82(3)					1.85
W(5)−O(58)	1.84(3)	W(6)−O(106)	1.95(3)					1.89
W(5)−O(15)	1.94(2)	W(6)−O(36)	1.93(2)					1.93
W(5)−O(25)	1.84(3)	W(6)−O(46)	1.87(3)					1.85
W(5)−O(112)	2.34(2)	W(6)−O(111)	2.34(2)					2.34
Si(1)−O(111)	1.62(2)	Si(1)−O(112)	1.69(2)					1.65
Si(1)−O(123)	1.58(3)	Si(1)−O(114)	1.60(3)					1.59
P(1)−O(100)	1.55(3)	P(1)−O(200)	1.48(3)	P(2)−O(300)	1.55(3)	P(2)−O(400)	1.49(3)	1.51
P(1)−O(1000)	1.50(4)	P(2)−O(2000)	1.49(4)					1.49
P(1)−C(1)	1.81(6)	P(2)−C(7)	1.80(5)					1.80
C(1)−C(2)	1.39(7)	C(3)−C(4)	1.23(9)	C(7)−C(8)	1.46(8)	C(9)−C(10)	1.43(8)	1.38
C(1)−C(6)	1.25(8)	C(4)−C(5)	1.5(1)	C(7)−C(12)	1.38(8)	C(10)−C(11)	1.39(9)	1.38
C(2)−C(3)	1.44(8)	C(5)−C(6)	1.46(9)	C(8)−C(9)	1.47(8)	C(11)−C(12)	1.40(9)	1.44

atoms	angle, deg	atoms	angle, deg	atoms	angle, deg	atoms	angle, deg	mean values, deg
W(2)−O(23)−W(3)	115.1(13)	W(1)−O(14)−W(4)	113.0(15)					114.0
W(2)−O(25)−W(5)	147.0(18)	W(1)−O(15)−W(5)	140.7(13)	W(4)−O(46)−W(6)	145.0(16)	W(3)−O(36)−(W(6)	138.2(13)	142.7
W(2)−O(28)−W(8)	140.3(17)	W(1)−O(17)−W(7)	142.1(16)	W(4)−O(104)−W(10)	142.3(17)	W(3)−O(39)−W(9)	143.2(16)	142.0
W(5)−O(58)−W(8)	124.5(15)	W(5)−O(57)−W(7)	121.5(12)	W(6)−O(106)−W(10)	118.1(14)	W(6)−O(69)−W(9)	121.8(14)	121.5
W(7)−O(107)−W(10)	160.7(14)	W(8)−O(89)−W(9)	166.5(15)					163.6
W(7)−O(78)−W(8)	123.1(14)	W(9)−O(109)−W(10)	122.0(14)					122.6
W(9)−O(111)−W(10)	92.6(8)	W(7)−O(112)−W(8)	93.6(8)					93.1
W(5)−O(112)−W(7)	91.5(8)	W(5)−O(112)−W(8)	91.4(8)	W(6)−O(111)−W(9)	90.3(8)	W(6)−O(111)−W(10)	91.2(7)	91.1
W(1)−O(114)−W(4)	95.5(9)	W(2)−O(123)−W(3)	92.1(9)					93.8
W(1)−O(100)−P(1)	136.1(19)	W(4)−O(200)−P(1)	137.1(18)	W(2)−O(300)−P(2)	133.1(15)	W(3)−O(400)−P(2)	136.5(18)	135.7
W(1)−O(114)−Si(1)	129.1(13)	W(4)−O(114)−Si(1)	127.6(13)	W(2)−O(123)−Si(1)	128.5(14)	W(3)−O(123)−Si(1)	126.8(15)	128.0
W(9)−O(111)−Si(1)	124.8(12)	W(10)−O(111)−Si(1)	126.0(12)	W(7)−O(112)−Si(1)	123.6(12)	W(8)−O(112)−Si(1)	124.5(13)	124.7
W(6)−O(111)−Si(1)	122.0(12)	W(5)−O(112)−Si(1)	123.1(12)					122.6

is shown in Figure 2. The anion is built up from a $[\gamma\text{-}SiW_{10}O_{36}]^{8-}$ unit and two phenylphosphonate ($PhPO^{2+}$) groups, which are linked to two oxygen atoms of two edge-shared WO_6 octahedra.

Although there are no crystallographic elements of symmetry through the hybrid anion, it adopts a geometry consistent with the symmetry of the $\{\gamma\text{-}SiW_{10}\}$ moiety i.e., C_{2v}. Actually the two phenyl rings are contained in a pseudomirror plane, orthogonal to the lacuna plane, which exchanges W_1, W_2, W_5, W_7, and W_8 in W_4, W_3, W_6, W_{10}, and W_9, respectively (Figure 3). Let us notice that, in the case of the phenylphosphonate derivatives of the monovacant Keggin anion $[PW_{11}O_{39}]^{7-}$, the phenyl rings are rotated by about $\pi/2$ and are oriented parallel to the plane defined by the lacunary surface of the polyanion.[8]

It is worth comparing the geometry of the SiW_{10} unit with that of the $[\gamma\text{-}SiW_{10}O_{36}]^{8-}$ precursor. For the central tetrahedron SiO_4, the $Si-O_a$ bond remains longer if the oxygen atom belongs to a tritungstic group (mean value 1.67 Å) than if it belongs to a ditungstic one (1.59 Å).

For simplification the tungsten atoms W(*i*) which become equivalent in the idealized C_{2v} symmetry will be given the

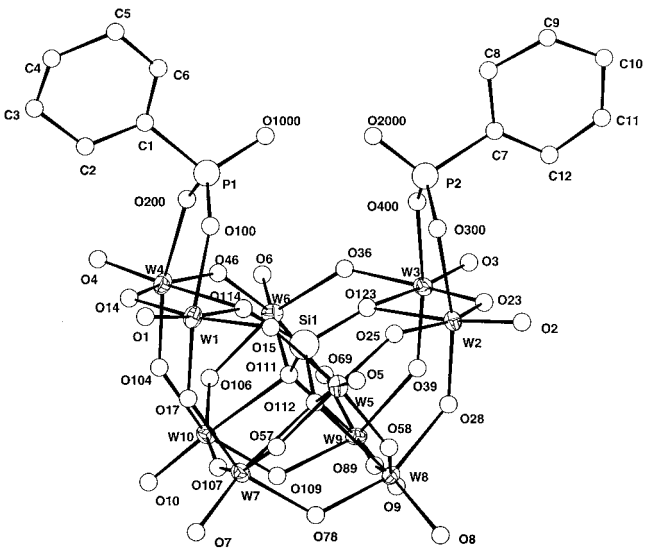

Figure 2. CAMERON view of $[\gamma\text{-}SiW_{10}O_{36}(PhPO)_2]^{4-}$ (**6**) with atom numbering according to IUPAC. Atoms are drawn at the 50% probability level.

(14) Pearce, L. J.; Watkin, D. J. *CAMERON;* Chemical Crystallography Laboratory: Oxford, U.K., 1994.

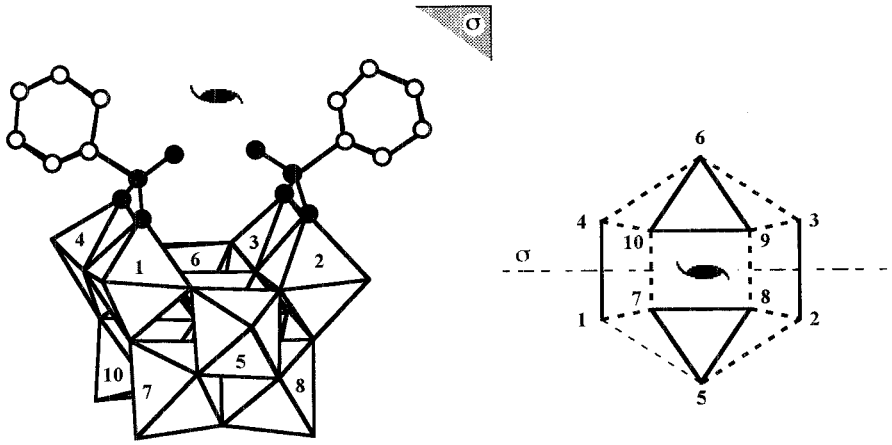

Figure 3. (a) Schematic representation of the $[\gamma\text{-SiW}_{10}O_{36}(PhPO)_2]^{4-}$ anion. (b) Schematic plane representation of the polytungstate framework. Edge and corner junctions are symbolized by solid and dotted lines, respectively.

Chart 1. Polyhedral Representation of $[\gamma\text{-SiW}_{10}O_{36}(PhPO)_2]^{4-}$ (Left) and (b) Focus on the W(A)−O−W(B)−O Junction (Right)

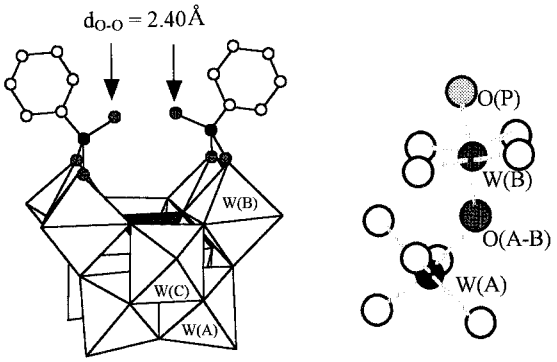

Table 4. Selected Bond Lengths and Mean Values (Å) for $[\gamma\text{-SiW}_{10}O_{36}(C_6H_5PO)_2]^{4-}$ (**6**) and $[\gamma\text{-SiW}_{10}O_{36}]^{8-}$

	6	mean	$[\gamma\text{-SiW}_{10}O_{36}]^{8-}$	mean
W(B)−O(P)[a]	1.99−2.03	2.02	1.70−1.79	1.74
W(B)−O(AB)	1.80−1.85	1.83	2.11−2.25	2.19
W(A)−O(AB	1.98−2.01	2.00	1.73−1.89	1.82

[a] O(P): μ-oxo bridging between W(B) and P in **6** and terminal atom in $[\gamma\text{-SiW}_{10}O_{36}]^{8-}$.

following symbolism:[9a] W(A) for $i = 7-10$, W(B) for $i = 1-4$, and W(C) for $i = 5$ and 6 (Figure 3 and Chart 1).

For the polytungstate shell, there is an increase of W(A)−O(AB) and W(B)−O(P) bonds and a decrease of W(B)−O(AB) bonds as compared with the lacunary $[\gamma\text{-SiW}_{10}O_{36}]^{8-}$ precursor (Table 4). In $\{\gamma\text{-SiW}_{10}\}$ the short W(B)−O(P) distance corresponds to a multiple bond between a tungsten atom and a terminal oxygen. By *trans* influence, the W(B)−O(AB) is elongated and correlatively the W(A)−O(AB) slightly shortened.

In the hybrid anion the terminal oxygen atom becomes a bridging atom, and it results in a lengthening of the corresponding W−O bond. By the effect of *trans* bond alternation, the W(B)−O(AB) is relatively shortened whereas on the contrary W(A)−O(AB) becomes elongated. It should be noticed however that the W(A)−O−W(B) angle remains at the same value in both $[\gamma\text{-SiW}_{10}O_{36}]^{8-}$ (143°) and $[\gamma\text{-SiW}_{10}O_{36}(PhPO)_2]^{4-}$ (142°).

Moreover the O−O distances between the two O(P) atoms belonging to the same dimetallic group are shortened in the phosphonate derivative (2.45 Å) with respect to that in the divacant starting anion (3.15 Å). Actually for the phosphonate species, this distance in the RPO_3 unit is very close to the O−O distance in a PO_4 tetrahedron of the Keggin anion.

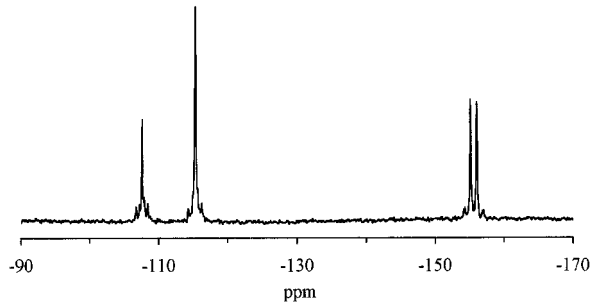

Figure 4. 12.5 MHz ^{183}W NMR spectrum of a 0.3 M solution of $[\gamma\text{-SiW}_{10}O_{36}(PhPO)_2]^{4-}$ (**6**) in DMF−acetone-d_6 (total acquisition time 14 h).

For the phosphonate groups, the O−O distance between both terminal oxygen atoms is remarkably short (d_{O-O} = 2.4 Å); such a short distance was already observed by Hill and co-workers for $[PW_{11}O_{39}(PhPO)_2]^{3-}$ (2.43 Å).[8] For two oxygen atoms very close to each other, one may anticipate a very strong hydrogen bond.[16] Unfortunately the X-ray structure determination does not allow one to determine the hydrogen atoms. However as only three cations, i.e. two NBu^{4+} and one NEt^{4+}, were located, the fourth cation must be a naked proton, likely "locked" between the two phosphoryl O terminal atoms.

When one considers the geometry of the trimetallic groups $W_5W_7W_8$ and $W_6W_9W_{10}$ the μ-oxo bridge between W(C) and W(A) is more open in $[\gamma\text{-SiW}_{10}O_{36}(PhPO)_2]^{4-}$ (mean value of W(C)−O−W(A) = 121.3°; Table 3) than in $[\gamma\text{-SiW}_{10}O_{36}]^{8-}$ (mean value 116.9°). Moreover the W(C)−O bond is significantly shorter in the hybrid derivative (mean value 1.87 Å) than in the lacunary precursor (mean value 1.94 Å).

^{31}P NMR Characterization. Under proton decoupling each ^{31}P NMR spectrum presents one resonance due to the RPO group (Figure S1, Supporting Information). This line displays satellites due to heteronuclear coupling ($^2J_{W-P} = 9-11$ Hz; see Experimental Section). Integration of these satellites with respect to the central line shows that each P atom is connected to two W atoms of the polyoxotungstate framework.[15] The chemical shifts for **2**−**4** and **6** and the $^2J_{W-P}$ coupling constants compare

(15) Thouvenot, R.; Tézé, A.; Contant, R.; Hervé, G. *Inorg. Chem.* **1988**, *27*, 524.
(16) Vinogradov, S. N.; Linnell, R. H. *Hydrogen Bonding;* Van Nostrand Reinhold Co.: New York, 1971.

Table 5. ^{183}W NMR Data[a] for [γ-$SiW_{10}O_{36}(RPO)_2$]$^{4-}$

referenced peak, assgnt	H	Et	*n*-Bu	*t*-Bu	C_2H_4COOH	Ph	multiplicity
C ($W_{5,6}$)	−106.2	−108.1	−108.7	−107.9	−107.9	−107.3	2
A (W_{7-10})	−114.3	−114.3	−114.9	−115.6	−116.1	−114.9	4
B (W_{1-4})	−152.6	−153.8	−155.4	−149.4	−153.7	−155.2	4
	(9.4)	(10.1)	(10.1)	(9.8)	(10.4)	(11.0)	

[a] Chemical shifts in ppm, $^2J_{W-P}$ in Hz in parentheses.

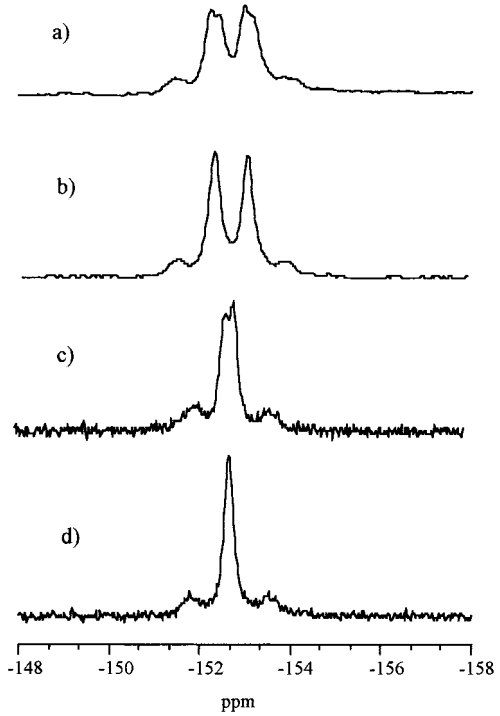

Figure 5. Expansion of the δ −152.6 line of the 12.5 MHz ^{183}W NMR spectrum of [γ-$SiW_{10}O_{36}(HPO)_2$]$^{4-}$ (**1**) in DMF−acetone-d_6: (a) undecoupled; (b) ^{1}H decoupled; (c) ^{31}P decoupled; (d) fully decoupled.

Table 6. ^{183}W Chemical Shifts/Coupling Constants Connectivity Matrix for [γ-$SiW_{10}O_{36}(PhPO)_2$]$^{4-}$ (**6**)[a]

referenced peak, assgnt	C	A	B
C ($W_{5,6}$)	−107.3	8.8	22.6
A (W_{7-10})	8.8	−114.9	24.8
B (W_{1-4})	22.6	24.8	−155.2

[a] Diagonal terms: chemical shifts, δ in ppm. off-diagonal terms: $^2J_{W-W}$ in Hz.

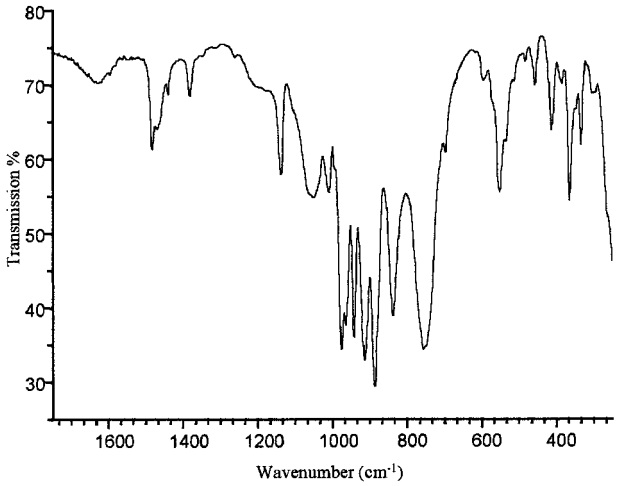

Figure 6. Part of the infrared spectrum ($\bar{\nu}$ < 2000 cm^{-1}) of $(NBu_4)_3$K-[γ-$SiW_{10}O_{36}(PhPO)_2$] (**6**), recorded in KBr pellets.

well with those of the phosphonate derivatives of the trivacant tungstophosphate with similar R group.[6]

^{183}W NMR Characterization. The ^{183}W NMR spectra of all species exhibit the same pattern of three resonances with relative intensity 1:2:2 (Figure 4 and Table 5).

In the solid state, the 10 tungsten atoms are independent, but in solution, the polyanion adopts the more symmetric conformation (C_{2v}) with three kinds of equivalent tungsten atoms of multiplicities 2:4:4. Each signal presents two pairs of satellites due to homonuclear tungsten−tungsten couplings, and the most shielded signal appears as a doublet due to heteronuclear phosphorus−tungsten coupling ($^2J_{W-P}$ = 9−11 Hz). These values are consistent with those observed by ^{31}P NMR spectroscopy (see above). In the case of **1** the most shielded resonance is a doublet of doublets (Figure 5) because of the long-range coupling with the proton of the PH group ($^3J_{W-H}$ = 2 Hz).

Generally, the complete assignment of ^{183}W spectra of polyoxotungstates requires the determination of tungsten connectivity by the mutual homonuclear coupling constants $^2J_{W-W}$.[17] In the present case the simplicity of the spectrum and the observation of the heteronuclear coupling allows one to assign very easily the resonance lines.

The high-frequency signal (≈−110 ppm) of relative intensity 1 is unambiguously assigned to W(C). The doublet at ≈−150 to −155 ppm corresponds necessarily to the W(B) atoms, which are linked to the organophosphonate group. The last signal at about −115 ppm is therefore assigned to W(A). This assignment is summarized in the chemical shift/coupling constants connectivity matrix presented in Table 6.

It is worth discussing the homonuclear coupling constants in both the lacunary {γ-SiW_{10}} anion and its organophosphonate derivatives. In the lacunary anion, the low corner coupling $^2J_{W(B)-W(A)}$ (4.9 Hz) was explained by the *trans* influence of the terminal oxygen atom O(P) of the lacuna (large W(B)−O(AB)). In the hybrid anion the O(P) atom links the phosphonate group to the tungsten W(B) atom, and it was shown above that the W(B)−O(AB) bond is considerably shortened. Consequently the ^2J coupling through the W(B)−O(AB)−W(A) bridge increases and exceeds 20 Hz, a value comparable to those in the saturated polyoxotungstates.[17] The other corner coupling, between W(B) and W(C), has nearly the same value in the lacunary (23.5 Hz) and the hybrid anion (22.6 Hz). Finally the edge coupling between W(A) and W(C) is markedly stronger in the phosphonate derivative ($^2J_{W-W}$ = 8.8 Hz) than in the divacant precursor ($^2J_{W-W}$ = 4.6 Hz). This can be discussed in the frame of the correlation between $^2J_{W-W}$ coupling constant and μ-oxo bridge angle.[17−19]Actually, because of increasing pπ−dπ overlap the ^2J coupling increases by opening the μ-oxo bridge, which is observed for [γ-$SiW_{10}O_{36}(PhPO)_2$]$^{4-}$ with

(17) Lefebvre, J.; Chauveau, F.; Doppelt, P.; Brévard, C. *J. Am. Chem. Soc.* **1981**, *103*, 4589.
(18) Contant, R.; Thouvenot, R. *Inorg. Chim. Acta* **1993**, *212*, 41.
(19) Thouvenot, R. *Acc. Chem. Res.*, submitted for publication.

Table 7. Infrared Data (cm^{-1}) for $(NBu_4)_3K[\gamma\text{-}SiW_{10}O_{36}(RPO)_2]$ and $[\gamma\text{-}SiW_{10}O_{36}]^{8-}$

assgnts[a]	H	Et	*n*-Bu	*t*-Bu	C_2H_4COOH	Ph	$\{\gamma-SiW_{10}\}$
$\nu_{as}(P-C)$		1152 vw	1178 vw	1173 vw	1171 vw	1137 vw	
$\nu_{as}(P-H)$	2436 vw						
$\nu_{as}(P-O)$	1070 w	1057 w	1062 w	1062 w	1065 w	1050 w	
$\nu_{as}(Si-O)$	1011 w	1008 w	1007 w	1008 w	1008 w	1010 w	989 w
$\nu_{as}(W=O_{ter})$	976 m	972 m	975 m	973 m	971 m	975 m	943 m
	964 m	959 m	963 m	962 m	966 m	964 m	
$\nu_{as}(W-O_b-W)$	941 s	946 s	943 s	940 s	943 s	942 s	906 s
	914 vs	906 vs	911 vs	912 vs	910 vs	914 vs	865 vs
	887 vs	877 vs	886 vs	885 vs	886 vs	887 vs	
	840 m	835 m	837 m	832 m	840 m	838 m	819 m
	761 vs	754 vs	756 vs	748 vs	760 vs	756 vs	744 vs
$\delta_{as}(Si-O_b)$	541 w	558 w	554 w	547 w	557 w	552 w	528 w
$\delta_{as}(W-O-W)$	415 m	409 m	418 m	415 m	413 m	412 m	395 sh
	364 m	361 m	364 m	363 m	363 m	364 m	360 m
	334 vw	333 vw	334 vw	334 vw	333 vw	334 vw	318 vw

[a] After ref 20.

respect to $[\gamma\text{-}SiW_{10}O_{36}]^{8-}$. Moreover, the shorter W(C)−O bond in the former compound is also responsible for a more efficient tungsten−tungsten spin−spin interaction.

Let us now comment on the ^{183}W chemical shifts. Although the tungsten atoms W(B) are the most concerned by the grafting of the RPO groups, their chemical shifts are nearly the same in both the lacunary and the derivatized tungstosilicates. On the contrary although far from the RPO groups, the W(C) nuclei are strongly deshielded, by more than 70 ppm, in the hybrid anion with respect to the lacunary one.

Infrared Spectra. Except the organic part, the infrared spectra of all compounds are very similar. A representative spectrum (**6**) is shown in Figure 6, and all data are given in Table 7. The low-wavenumber part ($\bar{\nu} < 1000$ cm^{-1}) is characteristic of the polyoxometalate framework.[20] The stretching vibrational bands [$\nu_{asym}(W-O_b-W)$ and $\nu_{asym}(W=O_{ter})$] are shifted to higher frequency as compared with those of the starting divacant anion $[\gamma\text{-}SiW_{10}O_{36}]^{8-}$ (Table 7). This effect is attributed to a saturation of the polyoxometallic moiety through the fixation of the RPO units.[4−6] Moreover, the complex pattern in the 420−300 cm^{-1} region is characteristic of the low symmetry of the γ isomer.[9a,13] The stretching vibrations of the RPO_3 groups are observed between 1000 and 1200 cm^{-1}. Moreover for **1** $\nu(P-H)$ stretching appears as a narrow band at 2436 cm^{-1}.

Conclusion

The reaction of $RPO(OH)_2$ with $[\gamma\text{-}SiW_{10}O_{36}]^{8-}$ leads to saturated organophosphonate derivatives, with retention of the structure of the polyoxotungstate framework, as confirmed by the crystallographic structure determination of $[\gamma\text{-}SiW_{10}O_{36}(PhPO)_2]^{4-}$ and by multinuclear NMR solution analysis. Obtention and characterization of these hybrid derivatives correspond to the first step toward preparation of oligomeric organic−inorganic species by reacting polyoxometalates with bis(phosphonate)s. This will be reported shortly.

Acknowledgment. We thank Dr. Jacqueline Canny for the preparation of generous amounts of the divacant $[\gamma\text{-}SiW_{10}O_{36}]^{8-}$ anion.

Supporting Information Available: Complete lists of final atomic positions (Table S1), anisotropic thermal parameters for the W atoms (Table S2), interatomic distances with esd's (Table S3), and bond angles with esd's (Table S4) and the $^{31}P\{^1H\}$ NMR spectrum of a mother solution of $[\gamma\text{-}SiW_{10}O_{36}(n\text{-}BuPO)_2]^{4-}$ (**3**) with abscissa expansion showing the tungsten satellites (Figure S1). This material is available free of charge via the Internet at http://pubs.acs.org.

IC990724F

(20) (a) Rocchiccioli-Deltcheff, C.; Thouvenot, R.; Franck, R. *Spectrochim. Acta, Part A* **1975**, *32*, 587. (b) Thouvenot, R.; Fournier, M.; Franck, R.; Rocchiccioli-Deltcheff, C. *Inorg. Chem.* **1984**, *23*, 598.